

Negative differential resistance in scanning tunneling microscopy: simulations on C₆₀-based molecular overlayers

Frederico D. Novaes¹, Manuel Cobian^{1,2}, Alberto García¹, Pablo Ordejón³, Hiromu Ueba⁴, and Nicolás Lorente³

¹ *Instituto de Ciencia de Materiales de Barcelona (CSIC), E-08193 Bellaterra, Spain*

² *LPMCN, UCBL, CNRS, UMR5586, 69622 Villeurbanne, France*

³ *Centre d'Investigació en Nanociència i Nanotecnologia (CSIC-ICN), E-08193 Bellaterra, Spain*

⁴ *Division of Nano Science, Graduate School of Science and Engineering, University of Toyama, Toyama, Japan*

(Dated: February 24, 2024)

We determine the conditions in which negative differential resistance (NDR) appears in the C₆₀-based molecular device of [Phys. Rev. Lett. **100**, 036807 (2008)] by means of ab-initio electron-transport simulations. Our calculations grant access to bias-dependent intrinsic properties of the molecular device, such as electronic levels and their partial widths. We show that these quantities depend on the molecule-molecule and molecule-electrode interactions of the device. Hence, NDR can be tuned by modifying the bias behavior of levels and widths using both types of interactions.

Since the creation of the first tunnel diode [1], a non-linear I - V characteristic, particularly showing negative differential resistance (NDR) is the cornerstone in two-terminal devices [2, 3]. NDR permits the electronic current of these devices to be modified by the applied bias in a complex way. This active control of the current motivates a long search for NDR in molecular devices [4–10] where the scanning tunneling microscope (STM) plays an important role [5, 6]. The STM can vary applied bias and tunneling current in an independent manner, yield atomically precise data and still be a two-terminal device. More recently, STM studies of C₆₀ molecules have spurred a lot of interest because of the NDR capabilities of C₆₀-based devices [8, 10–13].

As early as the first NDR cases were obtained in STM junctions, the existence of sharp resonances on both electrodes were used to explain the decrease of current as the bias increased [5, 6, 14]. However, Grobis and co-workers [11] explained their own NDR data by uncovering yet another mechanism: the voltage-dependent increase of the tunneling barrier height. Recently, one more mechanism has been advanced in order to explain the dependence of NDR on the tip's material, namely orbital matching between molecule and tip [15]. This last mechanism has been thoroughly studied and validated, while showing the need of sharp STM tips [16]. However, in most molecular devices, the accurate evaluation of the voltage drop across the device is crucial. As a matter of fact, Tu and co-workers [17] showed the paramount importance of the actual voltage-dependent barrier for the presence or absence of NDR. This spread of mechanisms shows that many parameters change among different molecular junctions and it is of fundamental importance to understand the key ingredients in NDR and thus the final functionality of possible molecular devices.

In this letter, we study the molecular device of Ref. [12] unraveling the mechanisms leading to the measured NDR [12]. The simulated molecular device consists of C₆₀ molecules partially decoupled from a Au (111) substrate by spectator 1,3,5,7-tetraphenyladamantane

(TPA) molecules. Despite the complexity of the simulations, we can extract the molecular levels and their coupling with the electrodes while describing their bias dependence. This allows us to have unprecedented insight in the actual physics of a molecular device with a quantitative description. We show that we can tune the size of the NDR signal by modulating the interplay of the bias dependence of the levels with the bias dependence of their partial widths which ultimately depend on molecule-molecule and molecule-electrode interactions.

In the Landauer formalism [18], the electronic current, I , is given in terms of the electron transmission function $T(E, V)$ with E the electron energy and V the applied bias (e and h being the electron charge and Planck's constant, respectively), by:

$$I = \frac{2e}{h} \int dE [f_R(E, V) - f_L(E, V)] T(E, V), \quad (1)$$

where the Fermi filling factors of the left and right electrodes, f_L and f_R include the bias, and correspond to the chemical potential of the left and right electrodes asymptotically inside each electrode. NDR corresponds to negative conductance. From Eq. (1), we can derivate with respect to the bias to obtain the conductance. We obtain two terms, one comes from the derivative of the Fermi filling factors and the other one corresponds to the derivative of the transmission. The derivative of the Fermi factors is a positive number, hence, only the derivative of the transmission gives rise to NDR. It is then, the behavior of the transmission function with bias that determines the appearance of NDR.

A quantitative way to compute Eq. (1) is to use non-equilibrium Green's functions (NEGF) self-consistently solved with Poisson's equations and fixed chemical potentials in the asymptotic region inside the electrodes. This has been done using the **Transiesta** package [19], where the electronic structure for the NEGF is evaluated using density functional theory (DFT) in the local density approximation (LDA). To optimize our calcula-

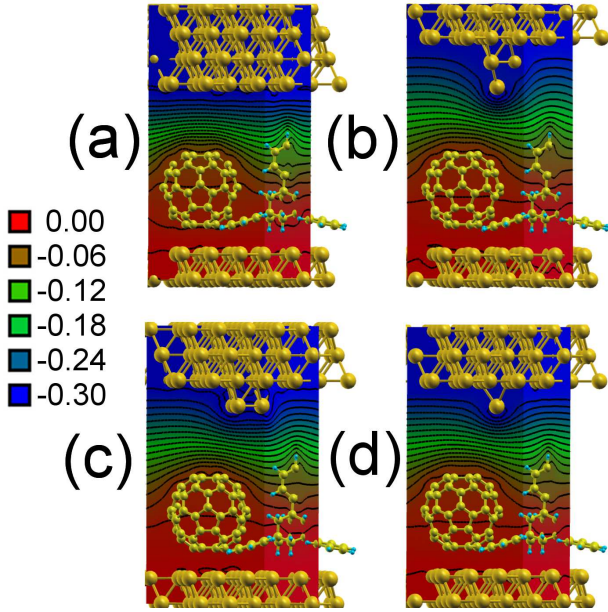


FIG. 1. Geometry and voltage drop for a 0.3-V bias in the four systems analyzed in this work: (a) a C_{60} -TPA overlayer on a semi-infinite Au(111) and a second semi-infinite Au(111) representing a flat STM tip, the tip-molecule distance is 6.7 Å, (b) the same overlayer under a pyramidal tip formed by 4 atoms and a semi-infinite Au(111) surface, the tip-molecule distance is 6.6 Å, the tip apex is off the center of the topmost C_{60} hexagon, (c) same as (b) but a capped pyramid with three atoms, the tip-molecule distance is 6.9 Å, (d) same as (a) plus a gold adatom, the tip-molecule distance is 6.9 Å, the tip apex is off the center of the topmost C_{60} hexagon. The voltage drop is shown on two planes cutting through the C_{60} and the TPA molecule respectively. The plotted isolines are 0.0083 V apart.

tions, we use a special surface basis-set that describe the electronic properties at the metal-vacuum interface [21]. Hence, the present electronic structure of the molecular overlayer on Au (111) reproduces the LDA results of Ref. [12]. The size of the electronic problem is very large since 5 active layers are used for right electrode, R , and four for the left one, L . Each layer contains 28 Au atoms [12]. The junctions include one C_{60} molecule and one TPA, plus the STM tip. Figure 1 shows the geometry and the voltage drop at the STM junctions considered in this work: (a) a flat tip, (b) a pyramide, (c) a capped one, and (d) an adatom. The atom-terminated tips are placed in a low-symmetry point over the C_{60} molecule, in order to avoid an unrealistic high-symmetry configuration. The two topmost layers of the R electrode and the topmost one of the L electrode are relaxed, the other three are fixed to the bulk position, and a recursion algorithm is used to reproduce semi-infinite electrodes [19] while allowing for the correct electric field screening and consequent Friedel oscillations.

Figure 1 also shows the voltage drop across the tunneling junction when the external bias is 0.3 V. We see

that most of the bias drop takes place in the vacuum region. At this bias, the LUMO [20] of C_{60} is close to the asymptotic chemical potential of the tip. Hence, C_{60} is largely conducting and the bias drop is smaller than in the vacuum gap: the voltage drops a tenth of the total bias just between the top of the molecule and the metallic substrate. The molecular states are then subjected to shift under the action of the bias. However, its partner TPA molecule has a large HOMO-LUMO gap which makes it basically inert. The voltage drop takes place across the molecule and it amounts to a seventh of the total bias. Hence, TPA behaves as the dielectric material of the molecular device that changes the charging energy of the active molecule, C_{60} . Calculations with and without TPA show that the charging energy of C_{60} is reduced by 0.2 eV in the presence of TPA. Finally, as the tip becomes sharper, the electric field gets more localized. As a consequence, the electric field is large close to the tip and the voltage drop is faster in the vacuum gap while smaller at the molecular site. Hence, by sharpening the tip we obtain an effect similar to increasing the vacuum gap which enhances the tunneling-barrier bias dependence [17].

The transmission behavior with applied bias varies rapidly as the tip changes. Figure 2 shows the electron transmission T of Eq. (1) as a function of the electron energy E , as the bias between tip and surface is increased. For a fixed bias, V , the transmission function can be reproduced by a Breit-Wigner [22] formula:

$$T(E, V) = \frac{\Gamma_R(V)\Gamma_L(V)}{(E - E_0(V))^2 + (\frac{\Gamma_R(V) + \Gamma_L(V)}{2})^2}. \quad (2)$$

The full-line curves in Fig. 2 are fits to Eq. (2) and dots are the **Transiesta**-evaluated transmissions. The agreement is excellent permitting us to extract the partial widths, Γ_R and Γ_L as well as the LUMO level E_0 as a function of applied bias, see Fig. 3.

The bias dependence of E_0 , Fig. 3, shows that the LUMO level is not pinned to the substrate's electronic structure because the bias is not entirely dropping in the vacuum gap. This is due to the molecule-molecule interactions of C_{60} with surrounding TPA, that decouple from the substrate and polarize C_{60} . The flat-tip causes the largest E_0 shift both at zero-bias and at finite bias, showing that despite the 6.7-Å vacuum gap, there is interaction between molecule and tip. The tip also modifies the coupling of the molecule with the substrate. Indeed, the partial width due to the substrate, Γ_R , can be divided in two values, Fig. 3, one corresponding to the blunt tips (a) and (c) and the other one to the atomic-like tips (b) and (d). Due to the stronger coupling of the molecule with the Au(111) substrate, Γ_R is larger and has a much smaller V -dependence than Γ_L that is the coupling with the tip. The behavior of Γ_R with V can be basically understood by the shift of the LUMO level, E_0 . As the

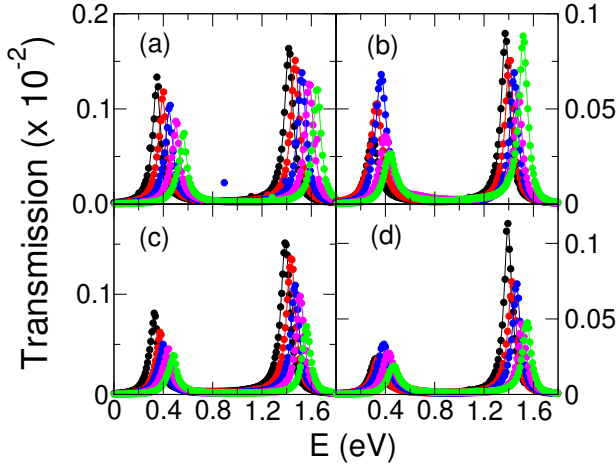


FIG. 2. Electron transmission as a function of the electron energy (E) the same junctions of Fig. 1: (a) the flat-tip junction (b) the pyramidal one (c) the capped one and (d) the adatom one. Filled circles are **TranSIESTA** results, and the full line is the fit to Eq. (2). The peaks shift with increasing bias, hence the lower-energy peak corresponds to 0.0 V, the next one to 0.4 V, 0.8 V, 1.2 V and 1.6 V respectively. Please, notice the different transmission scales on both sides.

bias increases, E_0 shifts closer to the vacuum level of the substrate, slightly increasing the partial width Γ_R . However, Γ_L is strongly dependent on the actual density of states (DOS) of the tip's electronic structure. Sharp tips, (b) and (d), show a non-monotonic behavior of Γ_L with V . This is also seen in the electron transmission since by virtue of Eq. (2), the transmission at E_0 is roughly proportional to Γ_L .

Figure 2 (a) is the transmission function for the flat tip case. We see that the transmission maximum, corresponding to the LUMO, shifts to higher energies as the bias is increased. This is due to the partial bias drop at the center of the molecule and is reproducing the behavior described in Ref. [17]. More interestingly, the maximum height drops with bias. This is the behavior described in Ref. [11] causing NDR. And indeed, as can be seen in Fig. 4 (a) NDR is found for this system. This fast decay of the transmission is due to the increase of the tunneling barrier with increasing bias [11, 17].

For the 4-atom pyramidal tip, Fig. 2 (b), the maximum of the transmission peaks when the bias is at ~ 0.8 V. This is totally different from the behavior of Fig. 2 (a) and the one described in Ref. [11]. The maximum of the transmission with bias can be traced back to a resonance of the 4-atom pyramidal tip of atomic origin. This is found at -0.45 eV in the DOS of the tip. Then, the strong variation of Γ_L with bias, Fig 3, is due to the resonance in the DOS. When the tip is capped, Fig. 1 (c), the corresponding Γ_L recovers a monotonic decrease with bias as for the flat-tip case (a), Fig. 3. Hence, the transmission is very similar to the case of the flat-tip. Finally, case (d) where one adatom is added to the flat

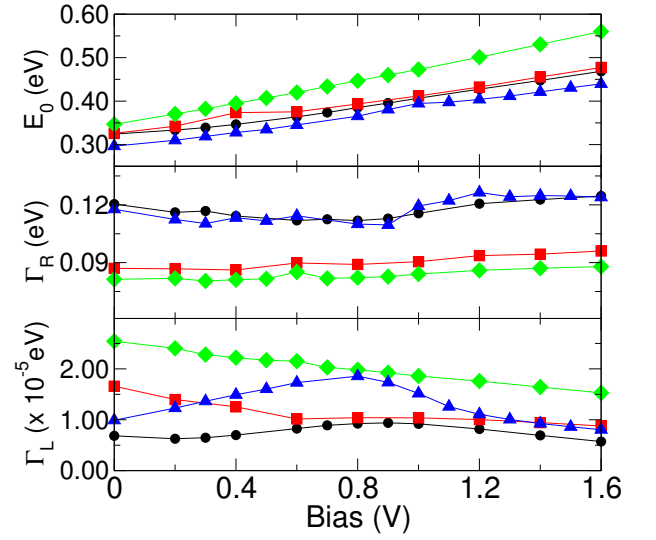


FIG. 3. Bias dependence of the LUMO level E_0 with respect to the substrate's Fermi energy, its partial width due to its coupling to the substrate, Γ_R and the partial width due to the coupling to the tip, Γ_L . Symbols: diamonds correspond to the flat tip of Fig. 1 (a), triangles to the 4-atom tip, (b), squares to the capped tip, (c), and dots to the adatom tip, (d).

tip shows the same kind of non-monotonic behavior in Γ_L as in (b) and a clear maximum in both, Γ_L and the transmission peaks for the LUMO around 0.8 V.

Figure 4 presents the I - V characteristics for the four systems of Fig. 1. The NDR features are large for the four-atom pyramidal tip, Fig. 4 (b) and small for the flat tip, Fig. 4 (a). Hence, the largest NDR is obtained when the partial widths present a resonant behavior with the applied bias, as the one due to electronic resonances in the electrodes, tip (b). The monotonic bias dependence of partial widths due to the barrier dependence on the bias, case (a), is slower leading to weak NDR. It is interesting to study the capped pyramidal tip, Fig. 4 (c), where NDR is absent and the I - V curve is closer to the flat-tip one. Here, the partial width dependence is slow, Fig. 3, with increasing bias because the tip's DOS is smoothly increasing. Despite the fact that the barrier height increases with bias, reducing the partial width, the increase of DOS is large enough to partially compensate the larger barrier and the transmission only drops slowly, Fig. 2 (c). NDR disappears. However, if one adatom is added to the flat tip, a bigger NDR effect is obtained because the sharper tip DOS forces a resonant-like Γ_L and hence a peak-shaped transmission. It is then this last effect, rather than the enhancing of the bias dependence of the tunneling barrier, Fig. 1, that drives NDR in sharp tips.

The shape of the I - V characteristics changes with tip. While the flat tip has a sharp onset and a sharp peak at 0.6 V, the atom-terminated tips have a broad peak

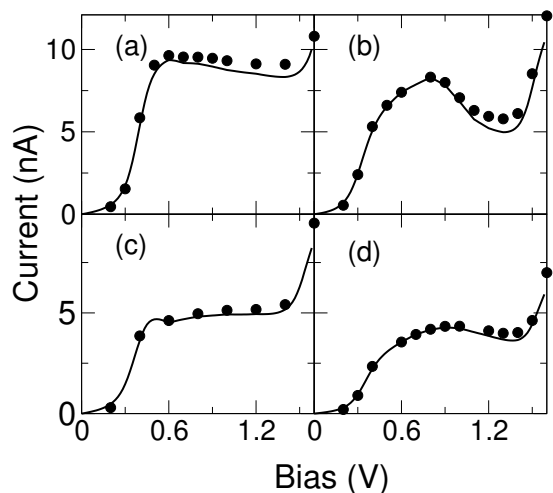


FIG. 4. I - V characteristics for the four cases studied here in the same order as Fig. 1. Dots are the *Transiesta* results, and full line the results of Eq. (1) using the Breit-Wigner fit, Eq. (2), interpolating the LUMO and LUMO+1 levels and partial widths for bias in between the *Transiesta* calculations. The fit excellently reproduces the LUMO onset in the current, however errors accumulate in between the LUMO and LUMO+1 onsets where the Breit-Wigner fit is worse. The current peak-to-valley ratios (dots) are (a) 1.07, (b) 1.4, (c) -, (d) 1.1, the experimental one [12] is 1.3.

centered at 0.8 - 0.9 V with a ~ 0.5 -V width. The experimental one is a broad peak centered at 1.1 V with a ~ 0.5 -V width [12]. This fact and the current peak-to-valley ratio, Fig. 4, render the pyramidal tip in very good agreement with the experiment. Moreover, the experimental distance between the LUMO and LUMO+1 onsets [12] is 1.5 V and the one in Fig. 4 is 1.2 V. The actual I - V shape is then determined by the bias dependence of the level, E_0 , and of the partial widths, here Γ_L . Indeed, the shape of, for instance, the LUMO onset is given by the V -dependence of E_0 [23], while the NDR drop is dominated by the V -dependence of Γ_L .

In summary, we have performed NEGF calculations for the experimental setup of Ref. [12]. Our simulations have permitted us to rationalize the appearance of NDR in this system in terms of molecular levels and partial widths because we have been able to extract their bias dependence. We have shown that NDR can be tuned by modifying molecule-molecule and molecule-electrode interactions. The molecule-molecule interactions induce a reduction of the overwhelming presence of the substrate permitting us to have molecular properties with sizeable bias

dependence. On the other hand, molecule-electrode interactions determine the molecular partial widths. NDR effects are maximum when the partial widths vary rapidly with the applied bias. This dependence is largest in the presence of electronic resonances on the electrodes such as the ones obtained for sharp STM tips. Finally, our results show that the overall shape of the I - V characteristic contains relevant information on the molecule-molecule and molecule-electrode interactions.

We thank K. J. Franke and J. I. Pascual for very interesting discussions. F.D.N acknowledges support from Juan de la Cierva program. Computing resources from CESGA and financial support from the Japanese JSPS, the Spanish MICINN (FIS2009-12721-C04-01), and the European ICT project "AtMol" are gratefully acknowledged.

-
- [1] L. Esaki, *Phys. Rev.* **109**, 603 (1958).
 - [2] L. Chang, L. Esaki and R. Tsu, *Appl. Phys. Lett.* **24**, 593 (1974).
 - [3] S. M. Sze, *Physics of Semiconductor Devices* (Wiley, New York, 1981), p. 190.
 - [4] A. Aviram and M. A. Ratner, *Chem. Phys. Lett.* **29**, 277 (1974).
 - [5] I. W. Lyo and P. Avouris, *Science* **245**, 1369 (1989).
 - [6] P. Bedrossian *et al.*, *Nature* **342**, 258 (1989).
 - [7] J. Chen *et al.*, *Science* **286**, 1550 (1999).
 - [8] C. G. Zeng *et al.*, *Appl. Phys. Lett.* **77**, 3595 (2000).
 - [9] M. Rinkio *et al.*, *ACS Nano* **4**, 3356 (2010).
 - [10] X. Zheng *et al.*, *ACS Nano* **4**, 7205 (2010).
 - [11] M. Grobis *et al.*, *Appl. Phys. Lett.* **86**, 204102 (2005).
 - [12] K. J. Franke *et al.*, *Phys. Rev. Lett.* **100**, 036807 (2008).
 - [13] I. Fernández Torrente, K. J. Franke, and J. I. Pascual, *J. Phys.: Condens. Matter* **20**, 184001 (2008).
 - [14] Y. Xue *et al.*, *Phys. Rev. B* **59**, R7852 (1999).
 - [15] L. Chen *et al.*, *Phys. Rev. Lett.* **99**, 146803 (2007).
 - [16] X.Q. Shi *et al.*, *Phys. Rev. B* **80**, 075403 (2009).
 - [17] X. W. Tu, G. Mikaelian, and W. Ho, *Phys. Rev. Lett.* **100**, 126807 (2008).
 - [18] R. Landauer, *IBM J. Res. Dev.* **1**, 223 (1957).
 - [19] M. Brandbyge *et al.*, *Phys. Rev. B* **65**, 165401 (2002); F. D. Novaes, A. J. R. da Silva and A. Fazzio, *Brazilian Journal of Physics*, **36**, 799 (2006).
 - [20] The LUMO of C_{60} is three-fold degenerate but there is only one LUMO contributing to the largest transmission eigenchannel.
 - [21] Sandra García-Gil *et al.*, *Phys. Rev. B* **79**, 075441 (2009).
 - [22] S. Datta, *Electronic transport in mesoscopic systems* (Cambridge University Press, Cambridge 1995).
 - [23] S. Díaz-Tendero *et al.*, *Nano Lett.* **8**, 2712 (2008).